Promotion of vesicular zinc efflux by ZIP13 and its implications for spondylocheiro dysplastic Ehlers–Danlos syndrome

Jeeyon Jeong[a,1], Joel M. Walker[a,1,2], Fudi Wang[a,3], J. Genevieve Park[b], Amy E. Palmer[b], Cecilia Giunta[c], Marianne Rohrbach[c], Beat Steinmann[c], and David J. Eide[a,4]

[a]Department of Nutritional Sciences, University of Wisconsin-Madison, Madison, WI 53706; [b]Department of Chemistry and Biochemistry, University of Colorado, Boulder, CO 80309; and [c]Connective Tissue Unit, Division of Metabolism, Children's Research Center, University Children's Hospital, CH-8032 Zurich, Switzerland

Zinc is essential but potentially toxic, so intracellular zinc levels are tightly controlled. A key strategy used by many organisms to buffer cytosolic zinc is to store it within vesicles and organelles. It is yet unknown whether vesicular or organellar sites perform this function in mammals. Human ZIP13, a member of the Zrt/Irt-like protein (ZIP) metal transporter family, might provide an answer to this question. Mutations in the ZIP13 gene, *SLC39A13*, previously were found to cause the spondylocheiro dysplastic form of Ehlers–Danlos syndrome (SCD-EDS), a heritable connective tissue disorder. Those previous studies suggested that ZIP13 transports excess zinc out of the early secretory pathway and that zinc overload in the endoplasmic reticulum (ER) occurs in SCD-EDS patients. In contrast, this study indicates that ZIP13's role is to release labile zinc from vesicular stores for use in the ER and other compartments. We propose that SCD-EDS is the result of vesicular zinc trapping and ER zinc deficiency rather than overload.

homeostasis | collagen

Zinc is an essential trace element. It serves as a catalytic or structural cofactor and mediates numerous metabolic processes. However, excess zinc is toxic. Therefore, intracellular zinc concentrations must be tightly maintained within a narrow optimal range. Cytosolic labile zinc in mammalian cells has been estimated to be at or below nanomolar concentrations (1, 2). Two metal transporter families, the SLC30A/cation diffusion facilitator (CDF)/zinc transporter (ZnT) family and the SLC39A/Zrt/Irt-like protein (ZIP) family, are primarily responsible for regulating zinc homeostasis in eukaryotes. ZnT proteins export zinc from the cytosol to outside the cell or into intracellular organelles, whereas ZIP transporters import zinc into the cytosol from the extracellular milieu or organellar lumen (3). The human genome encodes 10 ZnTs and 14 ZIPs, and the functions of many of them are still unclear.

Zinc is required in the cytosol and organelles, including those of the secretory pathway. Many zinc-dependent proteins reside in the secretory pathway, and others obtain this cofactor as they pass through the secretory system en route to their final destination. Resident zinc-requiring enzymes include the endoplasmic reticulum (ER)-localized chaperones calnexin and calreticulin (4) and GPI-phosphoethanolamine transferases (5, 6). Secreted zinc proteins include matrix metalloproteases (7), alkaline phosphatases (ALPs) (8), and angiotensin-converting enzymes (9). We previously showed that zinc is required for ER function. Both yeast and human cells experience ER stress when zinc deficient (10).

Among the ZnT proteins, ZnT5, ZnT6, and ZnT7 reside in the secretory pathway and transport zinc into the Golgi, whereas ZnT8 loads zinc into pancreatic secretory granules for insulin packaging (11, 12). Among ZIP family members, ZIP7 was found in the ER (13), and ZIP9 localizes to the Golgi (14), but their roles are not well understood.

ZIP13 is a member of the SLC39A/ZIP family (15). Recessive mutations in the ZIP13 gene, *SLC39A13*, were found to cause the spondylocheiro dysplastic form of Ehlers–Danlos syndrome (SCD-EDS) (16, 17). EDS is a group of heritable connective tissue disorders characterized by joint hypermobility, skin elasticity, and tissue fragility. Six different types of EDS have been identified, which generally are caused by mutations in collagen genes or genes involved in collagen modification or assembly (18).

SCD-EDS clinically resembles EDS type VI caused by mutations in the procollagen-lysine, 2-oxoglutarate 5-dioxygenase (*PLOD1*) gene encoding lysyl hydroxylase (LH1) (19). LH1 is an ER-resident enzyme responsible for procollagen hydroxylation on lysine residues (18). Lysine hydroxylation is required for cross-linking collagen fibrils for structural integrity. In addition to the overlapping clinical symptoms of SCD-EDS and EDS type VI, SCD-EDS patients show skeletal dysplasia and abnormalities of the hands. Interestingly, SCD-EDS–causing mutations were mapped to *SLC39A13* by two independent groups, and two of the authors of this study (C.G. and B.S.) previously had identified a deletion mutation in two family pedigrees (16). Subsequently, Fukada et al. (17) reported an amino acid substitution in ZIP13 from a third family and generated a *Slc39a13*^{−/−} knockout mouse that recapitulated the defects observed in the patients, thereby demon-

---

Significance

Intracellular zinc is tightly controlled because zinc is essential but potentially toxic. Many organisms regulate zinc using storage vesicles/organelles, but whether mammals do so is unknown. Here, we show that human ZIP13 releases zinc from vesicular stores. Previous studies found that mutations in the ZIP13 gene, *SLC39A13*, cause the spondylocheiro dysplastic form of Ehlers–Danlos syndrome (SCD-EDS) and speculated that ZIP13 exports zinc from the early secretory pathway and that zinc overload in the endoplasmic reticulum causes SCD-EDS. In contrast, our study suggests that SCD-EDS results from zinc deficiency in the endoplasmic reticulum resulting from zinc trapping in vesicular stores.

---

strating that mutations in *SLC39A13* cause SCD-EDS. SCD-EDS patients show normal collagen synthesis but decreased levels of collagen lysine and proline hydroxylation (16). Synthesis and posttranslational modifications of the nascent α-chains of collagen occur in the ER. The activities of lysyl and prolyl hydroxylases were not defective when assayed in SCD-EDS cell lysates (16). Because high zinc inhibits these hydroxylases in vitro, we proposed that impaired hydroxylation of lysyl and prolyl residues might be caused by ER zinc overload in SCD-EDS patients. Therefore, it was hypothesized that ZIP13 localized to the early secretory pathway and transported zinc out of the ER (16). This idea was supported by the observation that mouse ZIP13 protein was in the Golgi (17). It is likely that the zinc status of the Golgi and ER are closely linked by vesicular trafficking between those compartments.

Here we report our investigations of this hypothesis. We provide evidence that ZIP13 is indeed a zinc transporter. However, we show that, rather than localizing to the Golgi or ER, the endogenous human ZIP13 protein localizes to vesicles. Based on our results, we propose that ZIP13 is critical for zinc homeostasis by releasing labile zinc from vesicular stores for use in the ER and other compartments. Without functional ZIP13, as occurs in SCD-EDS, labile zinc becomes trapped in vesicles where it is unavailable for use elsewhere in the cell. Thus, we propose that the effects of *SLC39A13* mutations on collagen modification are the result of zinc deficiency rather than zinc excess in the early secretory pathway.

Results

ZIP13 Is a Zinc-Specific Transporter. To test if ZIP13 transports zinc, the protein was overexpressed in HEK293 cells, and zinc uptake was monitored. ZIP13 overexpression increased ^{65}Zn uptake compared with control cells (Fig. 1*A*). ZIP13-dependent zinc

uptake was concentration dependent and saturable with an apparent K_m of ~2 μM, similar to other mammalian ZIP transporters (20–22). It should be noted that this zinc transportation assay measures uptake across the plasma membrane, but endogenous ZIP13 normally resides on intracellular vesicles (see below). Thus, the activity detected here likely reflects that of mislocalized ZIP13, and we have noted that ZIP13 overexpression leads to accumulation of the protein in the plasma membrane.

To assess the substrate specificity of ZIP13, competition assays were performed with cells overexpressing ZIP13 in the presence of excess nonradioactive metal cations. Addition of 10- or 50-fold excess of nonradioactive zinc to cells overexpressing ZIP13 caused a marked decrease in ^{65}Zn uptake, whereas the presence of other metal ions did not have similarly strong effects (Fig. 1*B*). These results suggest that ZIP13 transports zinc specifically.

SLC39A13 Is Expressed in Many Tissues and Is Regulated by Zinc. Tissue-specific expression of *SLC39A13*, which encodes ZIP13, was examined by Northern blotting. *SLC39A13* was widely expressed among many human tissues tested (*SI Appendix*, Fig. S1). Expression was especially high in the heart, placenta, and skeletal muscle. We also detected *SLC39A13* expression in HeLa cells (Fig. 1*C*). To test whether *SLC39A13* was regulated by zinc, HeLa cells were grown in the presence of a zinc chelator, *N,N,N',N'*-tetrakis(2-pyridylmethyl) ethylenediamine (TPEN), and a range of zinc concentrations. Quantitative RT-PCR (qRT-PCR) analysis showed *SLC39A13* expression was elevated ~fivefold by severe zinc-limiting conditions (i.e., 5 μM TPEN) relative to that in basal medium (Fig. 1*C*). These results were consistent with the increased *Slc39a13* expression observed in tissues from zinc-deficient mice (23). Increased levels of ZIP13 protein also were observed under zinc-limiting conditions (Fig. 1*D*).
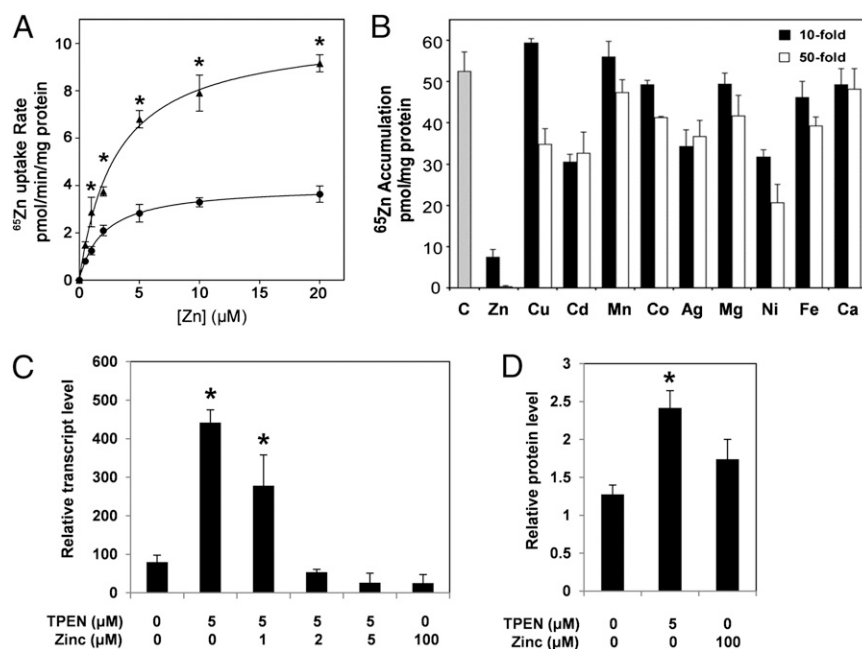
Fig. 1. ZIP13 is a zinc transporter, and *SLC39A13* expression is regulated by zinc. (*A*) Concentration-dependent zinc uptake (pmol·min^{-1}·mg protein^{-1}) in HEK293 cells overexpressing ZIP13 (▲) or vector-only control cells (●). $n = 3$; *$P < 0.05$. (*B*) Competition assays with HEK293 cells overexpressing ZIP13. ^{65}Zn accumulation (pmol/mg protein) was measured in the presence of 10- or 50-fold molar excess of the metals indicated. C, control with no metals added. All metals were divalent cations except for Ag(I). Each data point represents mean values from three independent experiments. The effect of added zinc was much greater than that of other metals ($P < 0.001$). Other metals found to have some effect in these assays ($P < 0.05$) were Cu, Cd, Co, Ag, Mg, Ni, and Fe. (*C*) *SLC39A13* expression under various zinc concentrations, with or without TPEN (12 h). Mean relative transcript levels detected by qRT-PCR are shown. $n = 4$; *$P < 0.05$. (*D*) Quantitation of ZIP13 protein levels under different zinc conditions. Untransfected HeLa cells were grown in basal medium or were treated for 12 h with 5 μM TPEN (low zinc) or 100 μM ZnCl$_2$ (high zinc). ZIP13 protein levels were detected by immunoblots and normalized with total protein. Mean values are shown. $n = 4$; *$P < 0.05$. Error bars indicate SE.

Thus, ZIP13 expression is regulated by zinc at the level of transcription and/or mRNA stability.

ZIP13 Localizes to Intracellular Vesicles. To determine the subcellular localization of endogenous ZIP13, immunofluorescence microscopy was conducted with HeLa cells using an anti-ZIP13 antibody. ZIP13 localized to punctate vesicles dispersed throughout the cytoplasm (*SI Appendix*, Fig. S2). Immunoblot and immunofluorescence analyses with anti-ZIP13 antibody pretreated with the ZIP13 antigen peptide or probed with the secondary antibody alone confirmed the specificity of anti-ZIP13 antibody (*SI Appendix*, Fig. S2 *A* and *B*). Immunofluorescence microscopy with other cell types, such as HEK293, HepG2, and primary dermal fibroblasts, revealed that the vesicular localization of ZIP13 is not unique to HeLa cells (Fig. 2*B* and *SI Appendix*, Fig. S2*C*). The vesicular distribution of ZIP13 was not noticeably affected by zinc status (*SI Appendix*, Fig. S3).

Vesicular localization of ZIP13 was confirmed using primary dermal fibroblasts from an SCD-EDS patient (P3/II) and from an unaffected heterozygous parent (M2/II) and siRNA-treated HeLa cells. Little ZIP13 protein was detected in fibroblasts from the SCD-EDS patient relative to the heterozygous control (Fig. 2*A*), and detection of ZIP13-containing vesicles in these cells also was reduced (Fig. 2*B*). The apparent molecular weight of ZIP13 detected by SDS/PAGE was lower than its expected molecular mass (35 kDa), likely because of the largely hydrophobic nature of the protein, its high capacity to bind SDS, and, therefore, its more rapid migration during gel electrophoresis (24). Transfecting HeLa cells with a pool of four siRNAs targeting ZIP13 decreased *SLC39A13* mRNA 10-fold (Fig. 2*D*) and also decreased punctate ZIP13 staining (Fig. 2*E*). Control experiments verified that ZIP13 siRNAs did not affect *SLC39A1* and *SLC39A7,* which encode related ZIP transporters (see *SI Appendix*, Fig. S5*A*). Also, two individual siRNAs from the pool of four were found to decrease *SLC39A13* mRNA and ZIP13 protein levels significantly when used alone (see *SI Appendix*, Fig. S5 *B* and *C*). These data strongly indicate a punctate vesicular distribution of endogenous ZIP13.

ZIP13 Does Not Colocalize with Many Known Organellar Markers. To identify the ZIP13 compartment(s), colocalization experiments were done with several well-characterized organellar markers. The punctate distribution of ZIP13 we observed was not consistent with the network-like structure of the ER. Furthermore, colocalization experiments with the ER markers CD3Δ-GFP and the KDEL receptor confirmed that ZIP13 is not abundant in the ER (Fig. 3). The mouse ortholog of ZIP13 and a V5-tagged allele of human ZIP13 previously were reported to localize to *trans*-Golgi (17, 25). However, endogenous human ZIP13 did not colocalize with the *trans*-Golgi marker, Golgin-97 (Fig. 3), and ZIP13 did not colocalize with markers for mitochondria, perox-
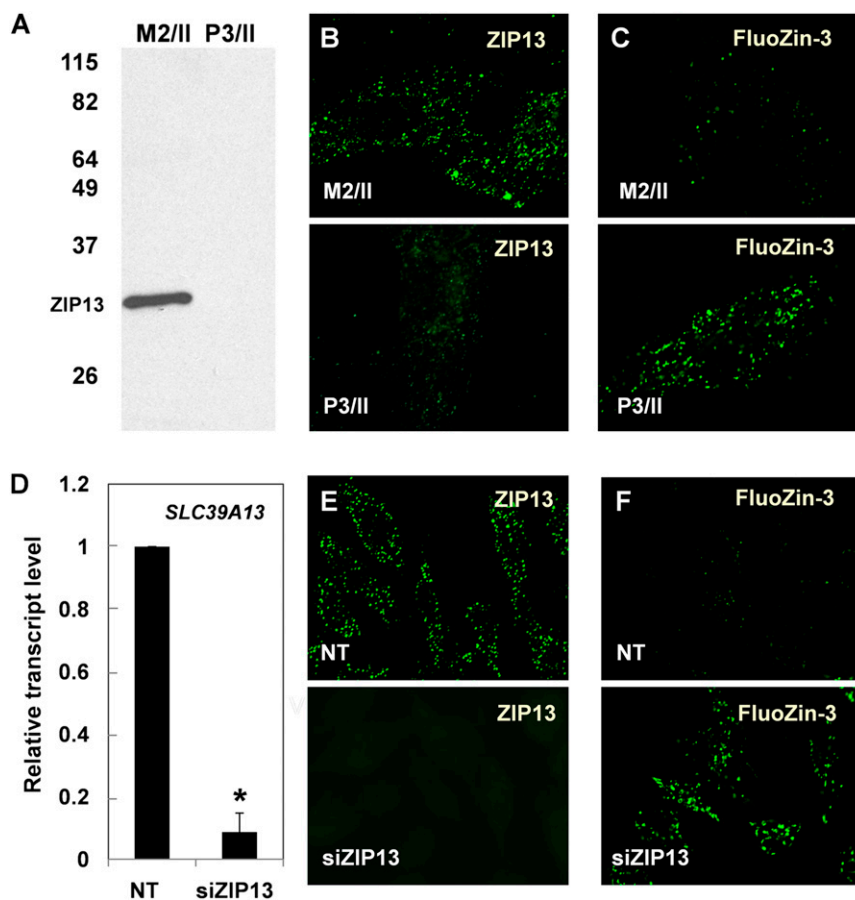

Fig. 2. Cells with loss of ZIP13 function. (*A*) Immunoblot with primary fibroblasts. Fibroblasts from an SCD-EDS patient (P3/II) and fibroblasts from a heterozygous parent (M2/II) were grown in basal medium, and total membranes were prepared for ZIP13 immunoblotting. (*B*) Immunofluorescence staining of ZIP13 in primary fibroblasts. M2/II and P3/II cells were grown under basal conditions and probed with anti-ZIP13 antibody. (*C*) FluoZin-3–stained images of primary fibroblasts showing labile zinc distribution. The cells were treated with 100 μM ZnCl$_2$ for 12 h before staining. (*D*) Expression of *SLC39A13* in HeLa cells treated with siRNA. HeLa cells were transiently transfected with nontargeting control siRNA (NT) or a pool of siRNAs targeting ZIP13 (siZIP13). Total RNA was isolated from the transfectants, and *SLC39A13* levels were detected by qRT-PCR. Mean values are shown. $n = 3$; *$P < 0.001$. Error bars indicate SE. (*E*) Immunofluorescence staining of ZIP13 in NT and siZIP13 HeLa cells. (*F*) FluoZin-3 staining of NT and siZIP13 cells treated as in *C*.
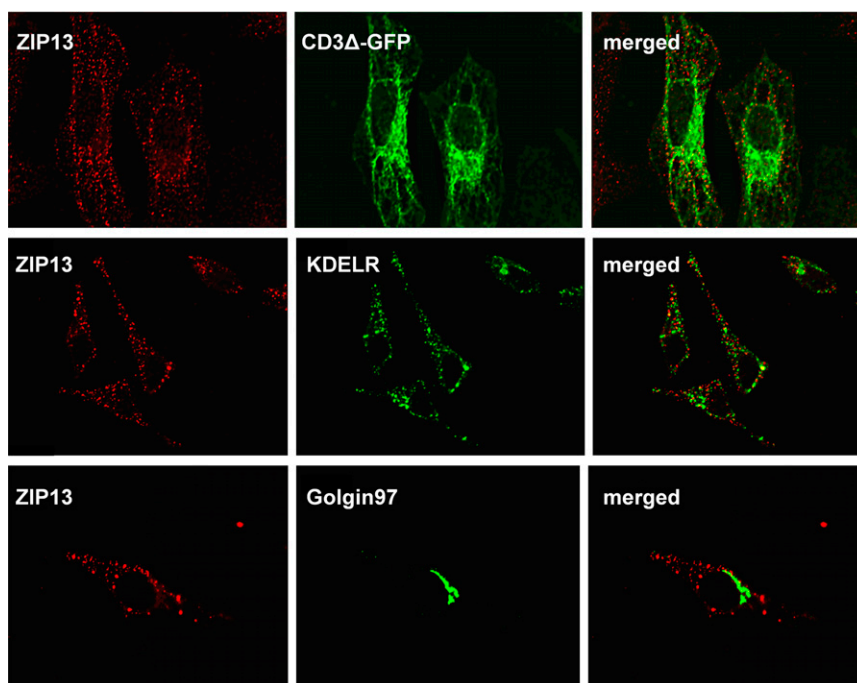
www.manaraa.com

Fig. 3. ZIP13 does not localize to the ER or Golgi. Immunofluorescence colocalization with ZIP13 (red) and ER (CD3Δ-GFP, KDELR) or Golgi (Golgin97) markers (green) in HeLa cells.

isomes, lysosomes, autophagosomes, early endosomes, late endosomes, or recycling endosomes, nor with vesicles bearing adaptins AP-1, -2, or -3 or the Rab4, 5, 7, 9, or 11 GTPases (*SI Appendix,* Fig. S4). Thus, despite extensive effort, the identity of ZIP13 compartment is unknown and appears to be unique.

Loss of ZIP13 Increases Vesicular Zinc. Human ZIP13 is not abundant in the ER or Golgi. Therefore, SCD-EDS symptoms are not likely to be caused by zinc excess in those compartments, as was proposed (16, 17). An alternative hypothesis arose from the observation that labile zinc accumulates in vesicles in mammalian cells (26, 27). The subcellular localization of ZIP13 and the regulation of *SLC39A13* mRNA levels by zinc status suggested a role for ZIP13 in mobilizing vesicular stores of labile zinc. Thus, we predicted that cells with reduced ZIP13 function would accumulate labile zinc within those vesicles. To test this prediction, HeLa cells transfected with nontargeting or ZIP13-targeting siRNA pools and primary fibroblasts from an SCD-EDS patient and a heterozygous parent were stained with a zinc-specific fluorescent dye, FluoZin-3, after treatment with high zinc. SCD-EDS is recessive, so the unaffected heterozygous parental cells provide a genetically related control for experiments addressing ZIP13 function. Interestingly, cells with decreased ZIP13, i.e., P3/II and siZip13, showed more FluoZin-3–stained vesicles and higher fluorescence intensity than their corresponding negative control cells (Fig. 2 *C* and *F*).

This pattern also was observed for HeLa cells treated with individual siRNAs (*SI Appendix,* Fig. S5D). FluoZin-3 staining with cells grown in basal medium revealed a less obvious but consistent pattern of more fluorescent vesicles in cells with reduced ZIP13 function (*SI Appendix,* Fig. S6). Zinc detection with Newport Green dichlorodihydrofluorescein diacetate (DCF), another zinc-responsive fluorophore, showed similar results, confirming that cells with reduced ZIP13 function had more vesicular labile zinc than control cells (*SI Appendix,* Fig. S7). Because of technical hurdles, it currently is unclear if ZIP13-containing vesicles and FluoZin-3/Newport Green DCF–stained compartments are the same (*Discussion*).

The apparent increase in vesicular zinc in cells with reduced ZIP13 function could indicate increased total zinc or changes in its intracellular distribution. Total cellular zinc levels measured by inductively coupled plasma mass spectrometry were not significantly affected in primary fibroblasts and siRNA-treated HeLa cells (*SI Appendix,* Fig. S8). Therefore, loss of ZIP13 function alters the distribution of cellular labile zinc but does not increase total accumulation.

Loss of ZIP13 Decreases Cytosolic Zinc. Vesicular localization of ZIP13 and redistribution of labile zinc in cells with reduced ZIP13 function suggested that the pathomechanism of SCD-EDS might be zinc deficiency in the secretory pathway caused by the trapping of labile zinc in vesicles. To test this idea, we first assessed the impact of decreased ZIP13 function on cytosolic zinc levels. We predicted that cells with decreased ZIP13 activity would have less cytosolic zinc. Expression of two metallothionein (MT) genes, *MT1a* and *MT2a*, is activated by elevated zinc (28). Therefore, their expression was examined in primary fibroblasts as an indirect measure of zinc status. qRT-PCR analysis showed that *MT1a* and *MT2a* expression was lower in fibroblasts from an SCD-EDS patient than in control cells grown in basal medium (Fig. 4 *A* and *B*). After high-zinc treatment, no significant difference between patient and control cells was observed, indicating that the differences in MT expression seen in basal medium were caused by zinc status and not by other factor(s) affecting MT expression.

MT genes are poorly expressed in HeLa cells (29). Therefore, we used a Zap1-based luciferase reporter as an indirect assay of cytosolic zinc. Zap1 is a zinc-responsive transcription factor from yeast, regulated by zinc binding directly to its two activation domains to inhibit their function (30). When Zap1 was fused to the DNA-binding domain of Gal4 (Gal4$_{DBD}$), zinc-responsive transcription in yeast was conferred on Gal4-regulated reporters (31). Zinc regulation of Gal4$_{DBD}$-Zap1 fusion also was found in HeLa cells expressing a GAL1^{UAS}-luciferase reporter. Reporter expression was elevated upon treatment with increasing concentrations of TPEN, whereas increased zinc reversed the
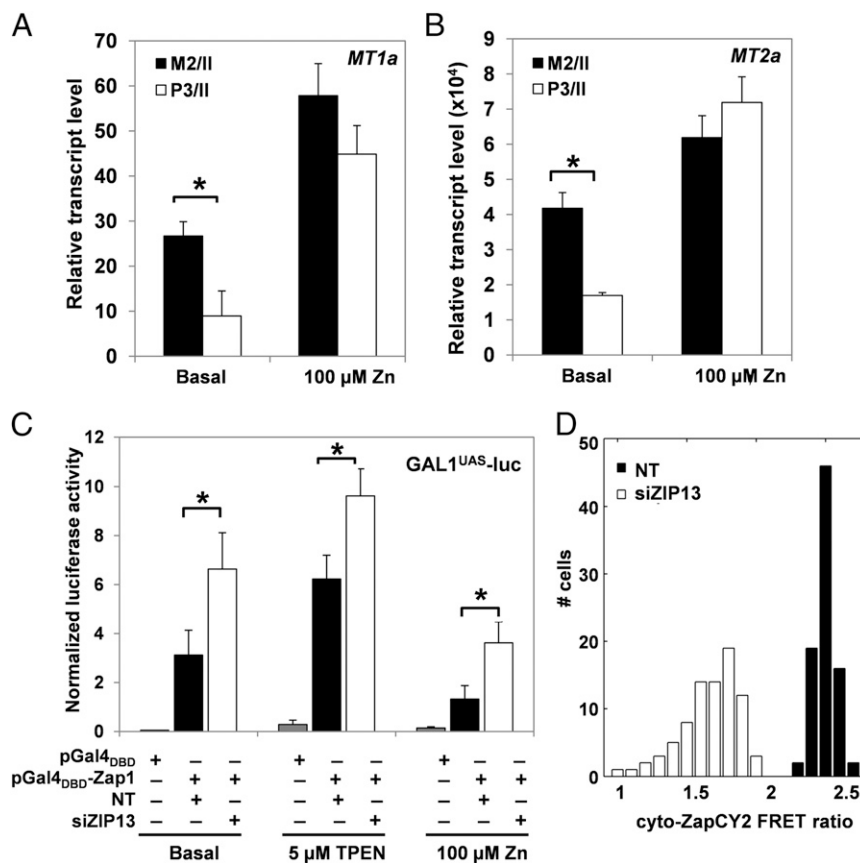
Jeong et al.

Fig. 4. Cytosolic zinc levels are decreased in ZIP13 loss-of-function cells. (*A* and *B*) Expression of *MT1a* (*A*) and *MT2a* (*B*) detected by qRT-PCR in primary fibroblasts. (*C*) Zap1-based reporter assays in HeLa cells cotransfected with GAL1^{UAS}-luciferase (firefly), *Renilla* luciferase, nontargeting (NT) or ZIP13-targeting (siZIP13) siRNAs, and pGal4$_{DBD}$-Zap1 or pGal4$_{DBD}$ alone and treated with different zinc conditions as indicated. Zap1-induced luciferase activity was normalized to *Renilla* luciferase and total protein. Mean values are shown. $n = 3$; *$P < 0.05$. Error bars indicate SE. (*D*) FRET ratio of siRNA-treated HeLa cells expressing cyto-ZapCY2 under basal conditions.

effect (*SI Appendix*, Fig. S9). These results indicated that the Gal4$_{DBD}$-Zap1 fusion can be used as a marker of zinc status in mammalian cells.

To examine cytosolic zinc in HeLa cells, siRNAs were cotransfected with the GAL1^{UAS}-luciferase reporter and a plasmid expressing either Gal4$_{DBD}$ alone or the Gal4$_{DBD}$-Zap1 fusion. These cells were grown in basal, low-zinc (5 μM TPEN), and high-zinc (100 μM Zn) media, and luciferase activity was assayed. Cells treated with ZIP13-targeting siRNAs showed higher luciferase activity than control cells under all conditions tested, suggesting that reduced ZIP13 function resulted in decreased cytosolic zinc (Fig. 4*C*). Increased zinc availability decreased luciferase activity, showing that the Gal4$_{DBD}$-Zap1 fusion was zinc responsive, but 100 μM zinc was not sufficient to restore cytosolic zinc in siZIP13 cells to control levels.

As a more direct assay, we used a recently developed fluorescent sensor, cyto-ZapCY2, to assess cytosolic zinc (2). ZapCY2 contains two zinc fingers (Znf1 and 2) from Zap1 sandwiched between enhanced cyan fluorescent protein (eCFP) and citrine fluorescent protein. When the sensor binds zinc ($K_d' = 811$ pM), it changes conformation, resulting in increased FRET from eCFP to citrine. The change in FRET can be detected by calculating the FRET ratio, which is the ratio of YFP (535 nm) to eCFP (475 nm) emission intensities upon excitation of eCFP (434 nm). Therefore, the FRET ratio is used as a reporter of labile zinc concentration. As shown (Fig. 4*D*), FRET ratios were substantially lower in HeLa cells transfected with ZIP13-targeting siRNAs grown in basal medium than in cells transfected with nontargeting siRNA (1.72 ±

0.21 vs. 2.55 ± 0.08, respectively; $P < 0.0001$). These results confirm observations from the indirect assays of MT expression and Zap1 activity that loss of ZIP13 function decreases cytosolic zinc.

Loss of ZIP13 Decreases Zinc in the Secretory Pathway. To determine if zinc trapping within vesicles causes zinc deficiency in the secretory pathway, we assayed the activity of ALPs. ALPs are zinc dependent and acquire zinc in the ER and/or Golgi (11). Because ALPs require zinc to be functional, their activity can reflect zinc levels in those compartments. We first measured ALP activity in primary fibroblasts. When grown in basal medium, fibroblasts from an SCD-EDS patient showed significantly less ALP activity than heterozygous control cells (Fig. 5*A*). After treatment with 5 μM TPEN, ALP activity was reduced dramatically in both cell types, highlighting the zinc dependence of ALP. When 50 μM zinc was added to the medium, ALP activity in the patient fibroblasts was not restored. However, when the cells were supplemented with 50 μM zinc and 5 μM pyrithione, a zinc ionophore, to improve zinc access to the ER and Golgi, ALP activity in patient fibroblasts was increased to that of control cells (Fig. 5*B*).

ALP activity also was measured in siRNA-treated HeLa cells. Because endogenous ALP activity in HeLa cells is low (*SI Appendix*, Fig. S10), the tissue-nonspecific alkaline phosphatase (TNAP) isozyme was overexpressed in these cells. Under basal conditions, TNAP activity was reduced significantly in cells treated with ZIP13-targeting siRNAs as compared with control cells (Fig. 5*C*). In both cell lines TNAP activity was reduced dramatically by treatment with 5 μM TPEN but was increased by zinc treat-
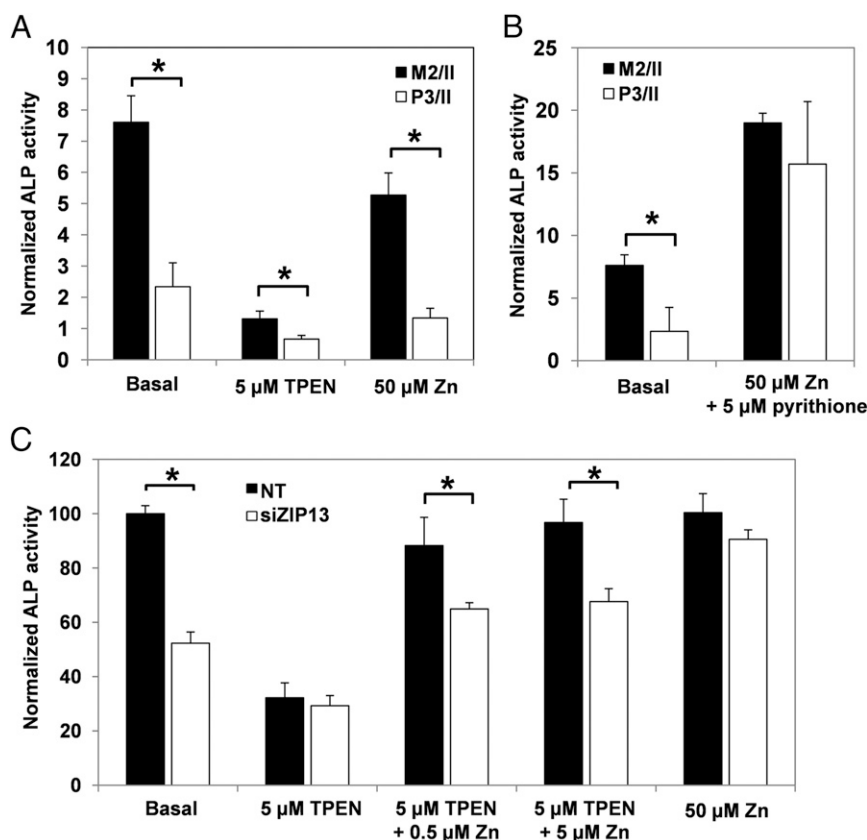
Fig. 5. Zinc status of the early secretory pathway. (*A* and *B*) Endogenous ALP activities in fibroblasts from a heterozygous patient (M2/II) and from an SCD-EDS patient (P3/II). Cells were grown in basal conditions or treated with TPEN and/or supplemented zinc with or without pyrithione for 12 h before the assay. (*C*) ALP activities in siRNA-treated HeLa cells overexpressing TNAP. Nontargeting (NT) or ZIP13-targeting (siZIP13) siRNA transfectants were grown in basal conditions or treated with combinations of TPEN and/or supplementary $ZnCl_2$ for 12 h before the assay. Mean values are shown. $n = 4$; *$P < 0.05$. Error bars indicate SE.

ment. Adding 50 μM zinc to the growth medium restored TNAP activity to control levels. These data are consistent with zinc deficiency in the early secretory pathway of cells with reduced ZIP13 expression.

Loss of ZIP13 Function Causes ER Stress. We showed previously that ER zinc deficiency disrupts ER function and induces ER stress (10). We therefore predicted that loss of ZIP13 function and the resulting loss of ER zinc caused by vesicular trapping would induce ER stress responses. To test this hypothesis, we used a luciferase reporter, 5xATF6-luciferase, that is responsive to the activity of the ER stress-responsive transcription factor, ATF6 (32). HeLa cells were cotransfected with the 5xATF6-luciferase reporter and either control or ZIP13-targeting siRNAs, and luciferase activity was measured. 5xATF6-luciferase expression showed a twofold increase in siZIP13-treated cells compared with control cells grown in basal or zinc-supplemented media (Fig. 6, *Inset*). Because supplementation of zinc did not restore 5XATF6-luciferase activity to control levels, we cotransfected the cells with a plasmid encoding ZnT7, which transports zinc into the early secretory pathway (11, 33). Because of variability in the results, it was unclear whether ZnT7 expression restored normal ATF6 activity. However, in control experiments with the ER stress inducer tunicamycin, we noted cells with reduced ZIP13 function were hypersensitive to the effects of this drug in inducing ATF6 activity (Fig. 6). This hypersensitivity phenotype also was not suppressed by high zinc alone but was rescued by coexpression of ZnT7. These results are consistent with increased ER stress in cells with reduced ZIP13 function that can be suppressed by transportation of zinc into the early secretory pathway.

Discussion

Mutations in *SLC39A13* recently were discovered to cause a variant form of EDS, SCD-EDS. We previously proposed that ZIP13 functions in the early secretory pathway to reduce ER zinc levels; without ZIP13 function, the secretory pathway becomes overloaded with zinc, which interferes with collagen modification by inhibiting lysyl and prolyl hydroxylases. We tested that model and report our results here. We show that ZIP13 is a zinc transporter, consistent with a recent finding that cells overexpressing V5 epitope-tagged ZIP13 accumulated more zinc than control cells (25). Competition studies also suggest that ZIP13 transports zinc with high preference over other metals.

Contrary to expectations, however, we did not find accumulation of human ZIP13 in the ER, as previously speculated (16), or in the Golgi, as observed for mouse ZIP13 (17). Instead, endogenous human ZIP13 is localized to punctate vesicles dispersed throughout the cytoplasm. Thus, our results suggest the primary site of ZIP13 action is not in the early secretory pathway but elsewhere in the cell. Notably, this conclusion does not contradict the observations of Fukada et al. (17); close examination of their immunofluorescence results show mouse ZIP13 localized on numerous cytoplasmic vesicles in addition to the Golgi. It is possible that mouse ZIP13 and the human protein localize slightly differently. Alternatively, the anti-mouse ZIP13 antibody may not have been completely specific for ZIP13 and possibly could have detected other proteins. Using ZIP13-targeting siRNAs and fibroblasts from an SCD-EDS patient, we confirmed the specificity of our antibody. With a V5 epitope-tagged ZIP13 allele, Bin et al. (25) localized the human protein to the Golgi and ER. However, mislocalization of this fusion protein is not surprising; we have found
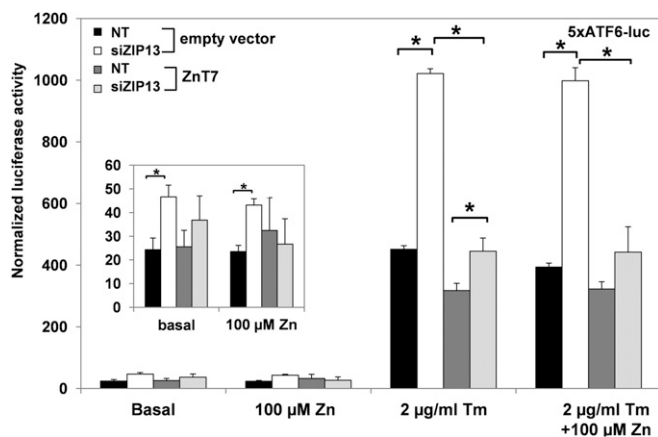
Jeong et al.

www.manaraa.com

Fig. 6. Induction of ATF6 activity in ZIP13 knockdown cells. HeLa cells were cotransfected with nontargeting (NT) or ZIP13-targeting (siZIP13) siRNA, 5xATF6-luciferase (firefly), and *Renilla* luciferase with or without ZnT7. Transfectants were treated with high zinc (100 μM ZnCl$_2$) and/or tunicamycin (Tm) 12 h before the assays. 5xATF6-luciferase activity was normalized to *Renilla* luciferase and total protein. *Inset* shows luciferase activity detected under basal and high-zinc conditions. Mean values are shown. $n = 3$; *$P < 0.05$. Error bars indicate SE.

that proper ZIP13 localization is very sensitive to both epitope tagging and expression levels.

The absence of human ZIP13 in the early secretory pathway led us to consider an alternative hypothesis of ZIP13 function. We proposed that the role of ZIP13 is to efflux labile zinc from vesicular stores (Fig. 7). According to this model, loss of ZIP13 function causes accumulation of zinc in those vesicles and depletes zinc from the cytosol, nucleus, and other compartments, including the ER. We tested this hypothesis in several ways using two different cell types, primary fibroblasts from an SCD-EDS patient and an unaffected heterozygous parent and HeLa cells transfected with ZIP13-targeting siRNAs or nontargeting control siRNA. Primary fibroblasts have the advantage of being a normal, nontransformed cell line. However, although parent and offspring cells are closely related, a major caveat is that they are not genetically identical, and this lack of identity could explain the variations observed between the two cell types. siRNA treatment of HeLa cells has the advantage of genetic homogeneity, albeit in a cell line that has been greatly altered from its normal state. Importantly, we obtained similar results from both cell types.

Consistent with our alternate hypothesis, loss of ZIP13 function caused the accumulation of labile zinc in vesicles. For technical reasons, it has not yet been possible to colocalize this labile zinc with ZIP13. Because permeabilization of cells disrupts labile zinc staining, immunofluorescence could not be used to colocalize labile zinc with ZIP13 by immunofluorescence microscopy. Extensive efforts to tag ZIP13 with fluorescent protein markers (e.g., tdTomato, mCherry) for this analysis were unsuccessful because these tags caused mislocalization of the fusion protein. Analysis of ZIP13-containing vesicles by proteomic methods may provide other markers more amenable to tagging that can be used to test this colocalization.

Also consistent with our hypothesis, we showed that zinc levels in the cytosol were decreased in cells with reduced ZIP13 activity. This decrease was shown with indirect assays (i.e., MT expression and Zap1 activity) as well as a direct FRET zinc sensor. MT expression is a widely used biomarker of intracellular zinc, and cytosolic and nuclear labile zinc pools are likely to be in equilibrium because of free diffusion through nuclear pores. Our use of the yeast Zap1 transcription factor as an assay for intracellular zinc in mammalian cells may be of use to other researchers in the zinc field. Because Zap1 is induced by zinc deficiency and

MTs are turned on by zinc excess, these two methods provide complementary assays to cover a broad range of zinc status.

Our prediction that zinc levels in the secretory pathway would be low rather than elevated was tested using ALPs as indicators of zinc status. ALP activities were low in cells with reduced ZIP13 function, and this defect was suppressed by high zinc. These results clearly refute the model of ER zinc overload and instead suggest the secretory pathway is zinc deficient. ER stress also was elevated in cells lacking full ZIP13 function and was suppressible by increasing available zinc. We attempted to use the ER-targeted ZapCY1 FRET sensor ($K_d' = 2.5$ pM) as a more direct measure of ER zinc (2) but did not detect a decrease in labile zinc in this compartment. One simple explanation for this paradox is that ER zinc is buffered at a very low level, and consequently under resting conditions the amount of sensor with zinc bound is less than 20% (2). Thus, the sensor is at its lower limit for detecting zinc, and decreases in labile zinc may not be detected readily. Alternatively, ALP/TNAP and ER-ZapCY1 might detect different pools of ER zinc. Nonetheless, the fact that no increase in ER zinc was observed with the FRET sensor indicates that loss of ZIP13 does not cause overload of labile ER zinc.

The hypothesis of secretory pathway zinc overload was supported by the detection of elevated levels of zinc in the Golgi of fibroblasts from *Slc39a13*$^{-/-}$ knockout mice using electron probe X-ray microanalysis (17). However, this result must be viewed with caution. The cells used for this analysis were fixed, stained, and embedded before analysis, and such manipulations are well known to cause loss and/or redistribution of diffusible elements (34). In addition, measuring elemental content using counts per second fails to account for background electron and X-ray scattering from mass thickness and the heavy metal stain used. Thus, the distribution of total zinc in these cells warrants reanalysis using improved methods.

This study supports the hypothesis that ER zinc deficiency underlies SCD-EDS. If so, how does that deficiency lead to the disease symptoms? One notable observation is that, although collagen hydroxylation is reduced in SCD-EDS patients, the activity of hydroxylase enzymes was normal or even elevated when assayed in lysates (16). Therefore, we propose the defects observed in
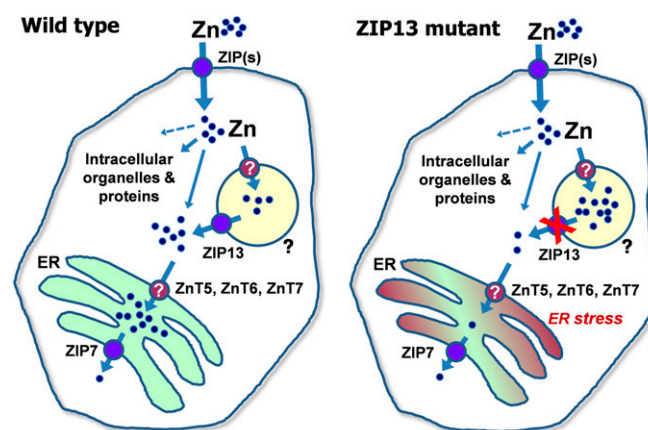

Fig. 7. Proposed model of ZIP13 function. ZIP13 localizes to vesicular sites that buffer cytosolic zinc levels to provide zinc for use in other compartments. Uptake into the ZIP13 compartment competes with uptake into other compartments and with utilization in the cytosol and nucleus. Cells with reduced ZIP13 function accumulate zinc in vesicles, causing zinc deficiency in the cytosol and other organelles, such as the ER, and leading to ER dysfunction and stress. Blue circles represent zinc ions, and the white question marks denote unknown zinc transporters. ZnT5, ZnT6, and ZnT7 likely contribute to zinc uptake into the ER, although they are primarily Golgi transporters. ZIP7, which is localized to the ER, transports zinc out of the ER. The relationship of the ZIP13 compartment (black question mark) to known organelles remains to be determined.

SCD-EDS patients are caused by a more general ER dysfunction rather than by the inhibition of hydroxylase activity per se. Collagen hydroxylation could be disrupted by reduced activity of ER resident chaperones such as calreticulin or DnaJ orthologs that require zinc for function; these proteins are known to play critical roles in collagen biogenesis (35). In support of this model, mouse embryonic fibroblasts that lack calreticulin were found to have reduced type I procollagen processing and extracellular matrix deposition (36). Collagen maturation may be one of many processes affected by vesicular zinc trapping and zinc deficiency in other compartments. Fukada et al. (17) noted defects in BMP/TGF-β signaling in Slc39a13⁻/⁻ knockout mice; these defects may be caused by zinc deficiency in the secretory pathway affecting surface receptor activity or low cytosolic zinc altering receptor-mediated signal transduction. For example, TGF-β–stimulated Smad2 nuclear translocation requires the zinc-dependent SARA protein (37).

Interestingly, many of the clinical features of SCD-EDS patients and phenotypes of Slc39a13⁻/⁻ knockout mice resemble symptoms of zinc deficiency in humans and animal models, such as growth retardation, decreased bone mineralization, and defects in collagen matrix formation (38–41). These similarities further support the model that the effects of ZIP13 mutations result from zinc deficiency in the ER and/or other compartments. These considerations suggest that providing zinc supplements to patients with SCD-EDS may have therapeutic benefits, and this notion could be tested using the Slc39a13⁻/⁻ knockout mice currently available (17).

A major unresolved question is the identity of the ZIP13 compartment. Endogenous human ZIP13 localized to cytosolic vesicles. Extensive efforts to colocalize ZIP13 with organellar marker proteins indicated that these vesicles were not the ER, Golgi, mitochondria, peroxisomes, autophagosomes, lysosomes, early endosomes, late endosomes, recycling endosomes, or vesicles bearing adaptin proteins AP-1, -2, or -3 or Rab4, 5, 7, 9, or 11 GTPases. Thus, the ZIP13 compartment appears to be unique. We currently are using proteomics to identify other components to characterize ZIP13-containing vesicles better.

Despite these remaining questions, our results suggest ZIP13 plays an important role in zinc homeostasis by controlling vesicular zinc storage. The observed increase in SLC39A13 mRNA and ZIP13 protein in zinc-limited cells is consistent with ZIP13 mobilizing zinc stores when cells are deficient. Organellar zinc storage sites have been discovered previously in yeast, plants, and, most recently, nematodes (42–44). The existence of vesicular zinc stores in mammalian cells has long been suggested by studies using zinc-staining fluorophores such as Zinquin or Newport Green. These probes consistently revealed that labile zinc is localized to vesicles dispersed throughout the cytoplasm of a large number of cell types (27, 45–50). These vesicles have been referred to as "zincosomes" because their relationship to known compartments was unclear (26, 51). Zincosomes were reported to be late endosomes (27, 52), but this result later was shown to be an experimental artifact (53). On the other hand, the ZIP13 vesicles may result from endocytotic events, given that many ZIP transporters reside on the plasma membrane (15). Nonetheless, the organellar identity of zincosomes is still unknown. Suggested roles for zincosomes in cellular zinc homeostasis include detoxifying excess zinc (27, 53), buffering cytosolic zinc from transient perturbations of zinc homeostasis (26, 49, 51, 54, 55), and storing readily accessible zinc for later use under zinc deficiency (54, 56). The zinc transporters that move zinc into and out of zincosomes also are unknown. We propose that ZIP13 is the transporter that is responsible for zinc efflux from this compartment. If so, ZIP13 will be a useful molecular tool with which to study the identity and function of vesicular zinc stores in mammalian cells.

Materials and Methods

Antibodies. A polyclonal antibody that recognizes human ZIP13 was generated against a peptide corresponding to residues 28–46 (RAGGSQPALRSRGTATAC) of ZIP13 in rabbits (Strategic BioSolutions). After the second bleed, the ZIP13-specific antibodies were purified using peptide bound to CNBr-Sepharose beads (GE Healthcare) following the manufacturer's protocol. A rabbit polyclonal antibody against a cytosolic loop of ZIP13 (Novus Biologicals) also was used in this study.

siRNA Transfection. HeLa cells were transfected with siGENOME SMART pool siRNA targeting SLC39A13 or siGENOME non-targeting siRNA at a final concentration of 25 nM using DharmaFECT Duo reagent (Dharmacon). For transfections with single siRNAs, a final concentration of 10 nM was used. All experiments were done 48 h after transfection.

FluoZin-3 Staining. Primary fibroblasts or siRNA-transfected HeLa cells were treated with 100 μM ZnCl$_2$ for 12 h before FluoZin-3 (Invitrogen) staining. FluoZin-3 stock solution (1 mM) was mixed with Pluronic F-127 [20% (wt/vol) solution in DMSO]; final concentration of 0.01% in staining medium] at a ratio of 2:1 immediately before use and then was added to Eagle's minimal essential medium (MEM) without serum to a final concentration of 1 μM FluoZin-3. The cells pretreated with high zinc were washed with PBS and stained for 1 h at 37 °C in a humidified CO$_2$ incubator, washed three times with PBS, and fixed with 4% (vol/vol) formaldehyde in PBS for microscopy. To ensure equal loading of FluoZin-3, cells were treated with high zinc in the presence of pyrithione before staining; no difference in staining intensity was observed (SI Appendix, Fig. S11). Informed patient consent was obtained for use of patient cells. The Health Sciences Institutional Review Board of the University of Wisconsin–Madison was responsible for overseeing the work with patients' cells.

Zap1-Based Luciferase Assays. HeLa cells were cotransfected with siRNA, pGal4-UAS luciferase (pG5luc; Promega), Renilla control (pRL-TK; Promega), and Gal4DBD-Zap1 fusion cloned in pcDNA3.1. In this construct, full-length Zap1 is fused to the Gal4 DNA-binding domain (31). Twenty-four hours after transfection, the cells were grown over a range of zinc levels, and a dual luciferase assay was conducted using the Dual Luciferase Reporter Assay system (Promega). Zap1-induced luciferase activity was normalized to Renilla luciferase and total protein.

5xATF6-Luciferase Assays. HeLa cells were cotransfected with siRNA, 5xATF6-GL3, and pRL-TK (Promega). Luciferase activity was measured by using the Dual Luciferase Assay kit (Promega) according to the manufacturer's directions. 5xATF6-luciferase activity was normalized to Renilla luciferase and total protein.

ALP Activity Measurements. HeLa cells were cotransfected with siRNA, a human TNAP cDNA clone (clone ID: 5752191) obtained from Thermo Scientific Open Biosystems, and pRL-TK (Renilla luciferase). For primary fibroblasts, endogenous ALP activity of the cells was measured. ALP assays were conducted following Suzuki et al. (11) with modifications. Total cellular protein extracts were prepared from cells lysed in lysis buffer [10 mM Tris·HCl (pH 7.5), 0.5 mM MgCl$_2$, 0.1% (vol/vol) Triton X-100] and were preincubated for 10 min at room temperature; then 100 μL of substrate solution [2 mg/mL p-nitrophenyl phosphate in 1 M diethanolamine buffer (pH 9.8), with 0.5 mM MgCl$_2$] was added to 10 μL of cell extracts. After incubation for 10 min at room temperature, ALP activity was measured based on the p-nitrophenol released by its absorbance at 405 nm, and the activity was normalized to Renilla luciferase and total protein. Shrimp ALP (Promega) was used as a standard.

FRET Zinc Sensors. HeLa cells grown in basal medium were cotransfected with siRNA and pcDNA3-ZapCY2 (GenBank JF261180.1). Cells were imaged at room temperature 48–52 h after transfection in HBSS supplemented with 20 mM Hepes, pH 7.4. Images were acquired on an Axiovert 200M inverted microscope (Zeiss) equipped with a xenon arc lamp (XBO75), a Cascade 512B CCD camera (Roper Scientific), a 40× plan-apo oil objective, and MetaFluor software (Molecular Devices). Microscope filter combinations used for FRET and CFP imaging are as follows: 430/24-nm excitation filter, 455-nm dichroic mirror, 535/25-nm (FRET) and 470/24-nm (CFP) emission filters. The mean FRET and CFP fluorescence intensity of each cell were calculated from acquired images using ImageJ software, and the mean background intensity was subtracted from these values before the FRET ratio was calculated. Cells expressing ~1–20 μM sensor were included in the analysis.

Jeong et al.

1. Vinkenborg JL, et al. (2009) Genetically encoded FRET sensors to monitor intracellular Zn2+ homeostasis. *Nat Methods* 6(10):737–740.
2. Qin Y, Dittmer PJ, Park JG, Jansen KB, Palmer AE (2011) Measuring steady-state and dynamic endoplasmic reticulum and Golgi Zn^{2+} with genetically encoded sensors. *Proc Natl Acad Sci USA* 108(18):7351–7356.
3. Lichten LA, Cousins RJ (2009) Mammalian zinc transporters: Nutritional and physiologic regulation. *Annu Rev Nutr* 29:153–176.
4. Leach MR, Cohen-Doyle MF, Thomas DY, Williams DB (2002) Localization of the lectin, ERp57 binding, and polypeptide binding sites of calnexin and calreticulin. *J Biol Chem* 277(33):29686–29697.
5. Sevlever D, Mann KJ, Medof ME (2001) Differential effect of 1,10-phenanthroline on mammalian, yeast, and parasite glycosylphosphatidylinositol anchor synthesis. *Biochem Biophys Res Commun* 288(5):1112–1118.
6. Mann KJ, Sevlever D (2001) 1,10-Phenanthroline inhibits glycosylphosphatidylinositol anchoring by preventing phosphoethanolamine addition to glycosylphosphatidylinositol anchor precursors. *Biochemistry* 40(5):1205–1213.
7. Chang C, Werb Z (2001) The many faces of metalloproteases: Cell growth, invasion, angiogenesis and metastasis. *Trends Cell Biol* 11(11):S37–S43.
8. Zurutuza L, et al. (1999) Correlations of genotype and phenotype in hypophosphatasia. *Hum Mol Genet* 8(6):1039–1046.
9. Turner AJ, Hooper NM (2002) The angiotensin-converting enzyme gene family: Genomics and pharmacology. *Trends Pharmacol Sci* 23(4):177–183.
10. Ellis CD, et al. (2004) Zinc and the Msc2 zinc transporter protein are required for endoplasmic reticulum function. *J Cell Biol* 166(3):325–335.
11. Suzuki T, et al. (2005) Zinc transporters, ZnT5 and ZnT7, are required for the activation of alkaline phosphatases, zinc-requiring enzymes that are glycosylphosphatidylinositol-anchored to the cytoplasmic membrane. *J Biol Chem* 280(1):637–643.
12. Chimienti F, et al. (2006) In vivo expression and functional characterization of the zinc transporter ZnT8 in glucose-induced insulin secretion. *J Cell Sci* 119(Pt 20):4199–4206.
13. Taylor KM, Morgan HE, Johnson A, Nicholson RI (2004) Structure-function analysis of HKE4, a member of the new LIV-1 subfamily of zinc transporters. *Biochem J* 377(Pt 1):131–139.
14. Matsuura W, et al. (2009) SLC39A9 (ZIP9) regulates zinc homeostasis in the secretory pathway: Characterization of the ZIP subfamily I protein in vertebrate cells. *Biosci Biotechnol Biochem* 73(5):1142–1148.
15. Jeong J, Eide D (2012) The SLC39 family of zinc transporters. *Mol Asp Med*, in press.
16. Giunta C, et al. (2008) Spondylocheiro dysplastic form of the Ehlers-Danlos syndrome—an autosomal-recessive entity caused by mutations in the zinc transporter gene SLC39A13. *Am J Hum Genet* 82(6):1290–1305.
17. Fukada T, et al. (2008) The zinc transporter SLC39A13/ZIP13 is required for connective tissue development; its involvement in BMP/TGF-beta signaling pathways. *PLoS ONE* 3(11):e3642.
18. Steinmann B, Royce PM, Superti-Furga A (2002) The Ehlers-Danols syndrome. *Connective tissue and its heritable disorders*, eds Royce PM, Steinmann B (Wiley-Liss, New York), pp 431–523.
19. Yeowell HN, Walker LC (2000) Mutations in the lysyl hydroxylase 1 gene that result in enzyme deficiency and the clinical phenotype of Ehlers-Danlos syndrome type VI. *Mol Genet Metab* 71(1-2):212–224.
20. Franklin RB, et al. (2003) Human ZIP1 is a major zinc uptake transporter for the accumulation of zinc in prostate cells. *J Inorg Biochem* 96(2-3):435–442.
21. Gaither LA, Eide DJ (2001) The human ZIP1 transporter mediates zinc uptake in human K562 erythroleukemia cells. *J Biol Chem* 276(25):22258–22264.
22. Wang F, Kim BE, Petris MJ, Eide DJ (2004) The mammalian Zip5 protein is a zinc transporter that localizes to the basolateral surface of polarized cells. *J Biol Chem* 279(49):51433–51441.
23. Lichten LA, Ryu MS, Guo L, Embury J, Cousins RJ (2011) MTF-1-mediated repression of the zinc transporter Zip10 is alleviated by zinc restriction. *PLoS ONE* 6(6):e21526.
24. Rath A, Glibowicka M, Nadeau VG, Chen G, Deber CM (2009) Detergent binding explains anomalous SDS-PAGE migration of membrane proteins. *Proc Natl Acad Sci USA* 106(6):1760–1765.
25. Bin BH, et al. (2011) Biochemical characterization of human ZIP13 protein: A homo-dimerized zinc transporter involved in the spondylocheiro dysplastic Ehlers-Danlos syndrome. *J Biol Chem* 286(46):40255–40265.
26. Haase H, Beyersmann D (1999) Uptake and intracellular distribution of labile and total Zn(II) in C6 rat glioma cells investigated with fluorescent probes and atomic absorption. *Biometals* 12(3):247–254.
27. Palmiter RD, Cole TB, Findley SD (1996) ZnT-2, a mammalian protein that confers resistance to zinc by facilitating vesicular sequestration. *EMBO J* 15(8):1784–1791.
28. Andrews GK (2001) Cellular zinc sensors: MTF-1 regulation of gene expression. *Biometals* 14(3-4):223–237.
29. Bittel D, Dalton T, Samson SL, Gedamu L, Andrews GK (1998) The DNA binding activity of metal response element-binding transcription factor-1 is activated in vivo and in vitro by zinc, but not by other transition metals. *J Biol Chem* 273(12):7127–7133.
30. Zhao H, Eide DJ (1997) Zap1p, a metalloregulatory protein involved in zinc-responsive transcriptional regulation in Saccharomyces cerevisiae. *Mol Cell Biol* 17(9):5044–5052.
31. Bird A, et al. (2000) Mapping the DNA binding domain of the Zap1 zinc-responsive transcriptional activator. *J Biol Chem* 275(21):16160–16166.
32. Wang Y, et al. (2000) Activation of ATF6 and an ATF6 DNA binding site by the endoplasmic reticulum stress response. *J Biol Chem* 275(35):27013–27020.
33. Kirschke CP, Huang L (2003) ZnT7, a novel mammalian zinc transporter, accumulates zinc in the Golgi apparatus. *J Biol Chem* 278(6):4096–4102.
34. LeFurgey A, Shelburne JD, Ingram P (1999) Preparatory techniques, including cryotechnology. *Biomedical applications of microprobe analysis*, eds Ingram P, Shelburne J, Roggli V, LeFurgey A (Academic, London), pp 59–85.
35. Lamandé SR, Bateman JF (1999) Procollagen folding and assembly: The role of endoplasmic reticulum enzymes and molecular chaperones. *Semin Cell Dev Biol* 10(5):455–464.
36. Van Duyn Graham L, Sweetwyne MT, Pallero MA, Murphy-Ullrich JE (2010) Intracellular calreticulin regulates multiple steps in fibrillar collagen expression, trafficking, and processing into the extracellular matrix. *J Biol Chem* 285(10):7067–7078.
37. Hayes S, Chawla A, Corvera S (2002) TGF beta receptor internalization into EEA1-enriched early endosomes: Role in signaling to Smad2. *J Cell Biol* 158(7):1239–1249.
38. Golub MS, et al. (1996) Adolescent growth and maturation in zinc-deprived rhesus monkeys [see comment]. *Am J Clin Nutr* 64(3):274–282.
39. Leek JC, et al. (1988) Long-term marginal zinc deprivation in rhesus monkeys. IV. Effects on skeletal growth and mineralization. *Am J Clin Nutr* 47(5):889–895.
40. Li Y, Yu ZL (2002) Effect of zinc on bone metabolism in fetal mouse limb culture. *Biomed Environ Sci* 15(4):323–329.
41. Kim JT, et al. (2009) Zinc-deficient diet decreases fetal long bone growth through decreased bone matrix formation in mice. *J Med Food* 12(1):118–123.
42. MacDiarmid CW, Gaither LA, Eide D (2000) Zinc transporters that regulate vacuolar zinc storage in Saccharomyces cerevisiae. *EMBO J* 19(12):2845–2855.
43. Ma JF, Ueno D, Zhao FJ, McGrath SP (2005) Subcellular localisation of Cd and Zn in the leaves of a Cd-hyperaccumulating ecotype of *Thlaspi caerulescens*. *Planta* 220(5):731–736.
44. Roh HC, Collier S, Guthrie J, Robertson JD, Kornfeld K (2012) Lysosome-related organelles in intestinal cells are a zinc storage site in C. elegans. *Cell Metab* 15(1):88–99.
45. Coyle P, et al. (1994) Measurement of zinc in hepatocytes by using a fluorescent probe, zinquin: Relationship to metallothionein and intracellular zinc. *Biochem J* 303(Pt 3):781–786.
46. Nasir MS, et al. (1999) The chemical cell biology of zinc: Structure and intracellular fluorescence of a zinc-quinolinesulfonamide complex. *J Biol Inorg Chem* 4(6):775–783.
47. Ho LH, Ratnaike RN, Zalewski PD (2000) Involvement of intracellular labile zinc in suppression of DEVD-caspase activity in human neuroblastoma cells. *Biochem Biophys Res Commun* 268(1):148–154.
48. Burdette SC, Walkup GK, Spingler B, Tsien RY, Lippard SJ (2001) Fluorescent sensors for Zn(2+) based on a fluorescein platform: Synthesis, properties and intracellular distribution. *J Am Chem Soc* 123(32):7831–7841.
49. St Croix CM, et al. (2002) Nitric oxide-induced changes in intracellular zinc homeostasis are mediated by metallothionein/thionein. *Am J Physiol Lung Cell Mol Physiol* 282(2):L185–L192.
50. Michalczyk AA, Allen J, Blomeley RC, Ackland ML (2002) Constitutive expression of hZnT4 zinc transporter in human breast epithelial cells. *Biochem J* 364(Pt 1):105–113.
51. Haase H, Beyersmann D (2002) Intracellular zinc distribution and transport in C6 rat glioma cells. *Biochem Biophys Res Commun* 296(4):923–928.
52. Kobayashi T, et al. (1999) Late endosomal membranes rich in lysobisphosphatidic acid regulate cholesterol transport. *Nat Cell Biol* 1(2):113–118.
53. Falcón-Pérez JM, Dell'Angelica EC (2007) Zinc transporter 2 (SLC30A2) can suppress the vesicular zinc defect of adaptor protein 3-depleted fibroblasts by promoting zinc accumulation in lysosomes. *Exp Cell Res* 313(7):1473–1483.
54. Kleineke JW, Brand IA (1997) Rapid changes in intracellular Zn^{2+} in rat hepatocytes. *J Pharmacol Toxicol Methods* 38(4):181–187.
55. Smith PJ, et al. (2002) DNA damage-induced [Zn(2+)](i) transients: Correlation with cell cycle arrest and apoptosis in lymphoma cells. *Am J Physiol Cell Physiol* 283(2):C609–C622.
56. Duffy JY, et al. (2001) A decrease in intracellular zinc level precedes the detection of early indicators of apoptosis in HL-60 cells. *Apoptosis* 6(3):161–172.

www.manaraa.com